Available online at www.sciencedirect.com

ScienceDirect

Procedia Engineering 67 (2013) 197 – 206

Procedia Engineering

www.elsevier.com/locate/procedia

7th Asian-Pacific Conference on Aerospace Technology and Science, 7th APCATS 2013

Linear Unsteady CFD of Vibrating Blades of Turbomachinery

H. Ishida[a,*], N. Yamasaki[a], M. Aotsuka[b]

[a]*Department of Aeronautics and Astronautics, Kyushu University, Fukuoka 819-0395, Japan*
[b]*Aero Engines and Space Operations, IHI Corporation, Tokyo 190-1297, Japan*

Abstract

This paper presents the numerical calculation of unsteady aerodynamic forces on the vibrating cascade blade row using the implicit time integration method. It is confirmed that first and second-order Euler methods, which are the implicit methods, require less computational time than the third-order Runge-Kutta method, which is the explicit method, by two orders of magnitude.

Keywords: CFD; Unsteady flow; Flutter; Aeroelasticity; Euler equation

1. Introduction

Flutter is one of the most serious concern of the aero-engine designers in the development of modern jet engines because it may cause fatal damages to jet engines. Therefore, the flutter analysis to evaluate accurately the unsteady aerodynamic forces on the vibrating cascade blades is essential. In the aero-engine component design processes, this evaluation of the flutter characteristics should be accelerated due to time constraint.

The paper presents the efficient method to compute numerically the unsteady aerodynamic forces on the vibrating annular cascade blades. The method is based on the linear unsteady formulation based on the finite volume method (FVM), the MUSCL (Monotone Upstream-centered Schemes for Conservation Laws) type, and the TVD (Total Variation Diminishing) scheme, following the UPACS (Unified Platform for Aerospace Computational Simulation) code developed by JAXA (Japan Aerospace Exploration Agency), Japan[1]. The linear unsteady calculation is effective in the design process of the turbomachinery as it requires less computational time compared with the fully unsteady (time-matching) calculation.

In order to reduce the computational time further, in the present paper, the implicit scheme (Matrix Free Gauss-Seidel, MFGS) is introduced instead of the explicit time integration scheme. The present paper is organized as

* Corresponding author. Tel.: +81-92-802-3019.
E-mail address: yamasaki@aero.kyushu-u.ac.jp

doi:10.1016/j.proeng.2013.12.019

follows: In Section 2, the implicit formulation is described. In Section 3, the numerical results and the computational time of the computational fluid dynamics (CFD) are compared between the implicit and explicit methods. Finally in Section 5, the conclusion is given.

2. Implicit Method for Linearized Euler Equations

The compressible Euler equations are given in the integral form as

$$\iiint Q_t dV + \oiint F dS = 0 \tag{1}$$

where $Q = [\rho, \rho u, \rho v, \rho w, E]^T$ denotes the, F denotes the inviscid flux vector, and S and V denote the surface area and volume of the control volume, respectively. Eq. (1) is linearized in the frequency domain as

$$\iiint \tilde{Q}_t dV + i\omega \iiint \tilde{Q} dV + \oiint \tilde{F} dS = 0 \tag{2}$$

where $\tilde{Q} = [\tilde{\rho}, \tilde{\rho}u + \rho\tilde{u}, \tilde{\rho}v + \rho\tilde{v}, \tilde{\rho}w + \rho\tilde{w}, \tilde{E}]^T$ denotes the linear-unsteady conservative variable vector, $\tilde{F}$ denotes the linear inviscid flux vector, and ω denotes the angular frequency. In the linear unsteady formulation, the time averaged steady variables are solved by Eq. (1) with a time marching method, and the time dependent unsteady variables are solved by Eq. (2) with the time marching method in pseudo time t. For details, see Ref. [1].

In the present paper, the implicit methods are introduced to the formulation in order to reduce the calculation time, so the implicit formulation of Eq. (2) is discussed here. The method adapted here is the MFGS method[2]. The delta form (time incremental form) of equation is given by

$$V_i\left(\frac{1}{\Delta t_i} + i\omega\right)\Delta\tilde{Q}_i + i\omega V_i \tilde{Q}_i^n + \sum_j \tilde{F}_{ij} S_{ij} = 0, \qquad \Delta Q_i = Q_i^{n+1} - Q_i^n \tag{3), (4}$$

where i denotes the cell index of the control volume, and ij denotes the interface of the cell i and the adjacent cell j. The superscript n denotes the time step.

The LU-SGS (LU Symmetric Gauss-Seidel) formulation of Eq. (2) is given by

$$\Delta\tilde{Q}_i^* = \left(V_i\left(\frac{1}{\Delta t_i} + i\omega\right) + \sum_j S_{ij} A_{ij}^+\right)^{-1}\left[\sum_{j\in\text{Lower}} S_{ji} A_{ji}^+ \Delta\tilde{Q}_j^* - \sum_j \tilde{F}_{ij} S_{ij} - i\omega V_i \tilde{Q}_i^n\right], \tag{5}$$

$$\Delta\tilde{Q}_i^{n+1} = \Delta\tilde{Q}_i^* + \left(V_i\left(\frac{1}{\Delta t_i} + i\omega\right) + \sum_j S_{ij} A_{ij}^+\right)^{-1} \sum_{j\in\text{Upper}} S_{ji} A_{ji}^+ \Delta\tilde{Q}_j^* \tag{6}$$

where A^+ is the part of the Jacobian matrix corresponding to the positive eigenvalue. Note that the Jacobian matrix $A = \partial F / \partial Q$ remains the same in the unsteady formulation. Here the Jameson-Turkel approximation

$$A_{ij}^{+} = \frac{A_{ij} + \sigma_{ij} I}{2}, \tag{7}$$

is introduced, where σ_{ij} is the spectral radius (the largest eigenvalue of the Jacobian matrix) and I is the unit matrix. This approximation enables the matrix inversion. Eq. (6) is simplified by this approximation as follows:

$$\Delta\tilde{Q}_i^{n+1} = \left[\sum_{j \in \mathrm{Lower}} S_{ji} A_{ji}^{+} \Delta\tilde{Q}_j - \sum_j \tilde{F}_{ij} S_{ij} - i\omega V_i \tilde{Q}_i^n \right] / \left(V_i \left(\frac{1}{\Delta t_i} + i\omega \right) + \sum_j S_{ij} \frac{\sigma_{ij}}{2} \right). \tag{8}$$

This formulation is frequently called LU-SGS implicit method. Incidentally, the Jacobian matrix can evaluated numerically in a matrix-free form as

$$A_{ji}^{+} \Delta\tilde{Q}_j = \frac{\hat{E}_{ji}(\tilde{Q}_j^n + \Delta\tilde{Q}_j) - \hat{E}_{ji}(\tilde{Q}_j^n) + \sigma_{ji} \Delta\tilde{Q}_j}{2}. \tag{9}$$

By making use of $\tilde{Q}_i \approx \tilde{Q}_j$, Eq. (9) is reduced to

$$\sum_j S_{ij} A_{ji}^{+} \Delta\tilde{Q}_j = \sum_j S_{ij} \frac{\hat{E}_{ji}(\tilde{Q}_i^n + \Delta\tilde{Q}_j) + \sigma_{ij} \Delta\tilde{Q}_j}{2}. \tag{10}$$

3. Numerical Results and Discussion

3.1. Solver

After the original UPACS solver is used to calculate the steady (time-mean) flow, which is based on the FVM formulation using the MUSCL type, and TVD, the linear unsteady solver which is the modified version of the original UPACS.

3.2. Annular Helical Cascade Blade Model with No Steady Loading

At first, the annular helical cascade blade model with no steady loading[3] is discussed. The number of blades is N = 30, the hub/casing diameter ratio h = 0.4, the non-dimensional rotating speed Ω_z = 2.4744, and the stagger angle ξ = 67.49 degrees. The vibration mode is the bending mode, the non-dimensional amplitude A = 1.0×10^{-4}, the non-dimensional angular frequency ω = 0.9, and the interblade phase angle IBPA = 72 degrees. The numerical grid is shown in Fig. 1. The number of grids is 21×31×106.

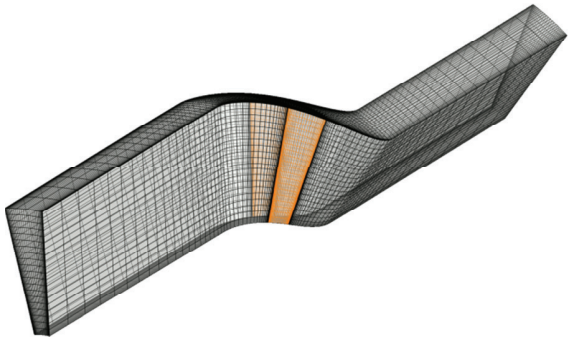

Fig. 1 Grids for Annular Helical Cascade Blade Model with No Steady Loading

Table 1 shows the computational time in hours required for the solution to converge to the same convergence criterion (residual reaches 10^{-9}) using the third-order Runge-Kutta method as the explicit time integration method, and the first and second-order Euler methods as the implicit time integration methods. Note that in the first and second-order Euler methods, the sub-iteration number of the smallest computational time is adopted, and its sub-iteration number and the computational time are shown. For example, CFL = 10→50 denotes that the iteration starts at CFL = 10, CFL is increased proportionally as CFL = 1.2 $CFL_{last\_iteration}$ until CFL reaches the maximum of CFL = 50.

Table 1 Comparison of the computational time in hours

	CFL Number			
Time Integration Method	0.1 → 0.5	10 → 50	20 → 100	50 → 250
Third-order Runge-Kutta	63.43	-	-	-
First-order Euler	-	1.28, 2	1.01, 2	0.84, 2
Second-order Euler	-	4.06, 4	5.28, 14	6.15, 22

From Table 1, the computational time is 63.43 hours when the third-order Runge-Kutta method is used, while it is 0.84 hours when the first-order Euler method is used with CFL = 50→250 and 4.06 hours when the second-order Euler method is used with CFL = 10→50. By using the implicit methods, the computational time is reduced approximately by 1/75 and 1/15 when the first and second-order Euler methods are used, respectively.

Figures 2 and 3 shows the comparison of the unsteady pressure difference between the pressure and suction surfaces using the explicit and first-order Euler implicit methods on the four radial cross-sections from the hub (ΔR = 0.4) to casing walls (ΔR = 1.0). The real part is in phase with the vibration amplitude, and the imarinary part is out of phase. As is shown in Figs. 2 and 3, the correspondence of the numerical results using the explicit and first-order Euler implicit methods is superb.

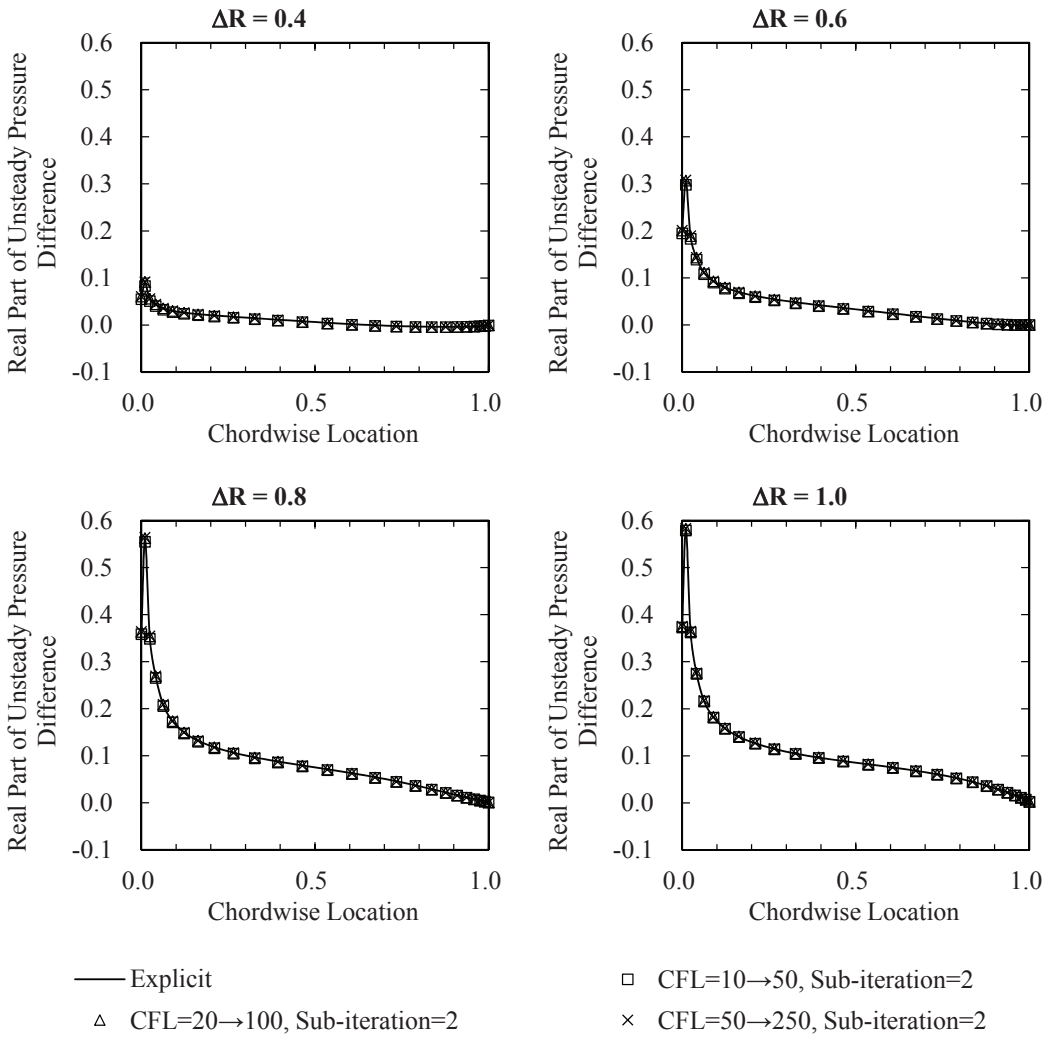

Fig. 2 Comparison of the real part of unsteady pressure difference using the explicit and first-order Euler implicit methods

Thus, switching the time integration method from the explicit method to the implicit method, the first-order Euler method in this case, enables the reduction in the computational time. It should be noted that the second-order Euler implicit method still gives the same results (omitted due to the limited space of the paper), but the usage of the second-order Euler implicit method requires about five times as much time as the usage of the first-order Euler method.

3.3. Low Pressure Turbine Model

The low pressure turbine model modified slightly from the proprietary production model is discussed next. Although it is two-dimensional, the strong steady flow makes the computation severe. Figure 4 shows the numerical grids. The number of grids is 101×81×3.

Table 2 shows the computational time in hours required for the solution to converge to the same convergence criterion (residual reaches 10^{-6}) using the third-order Runge-Kutta method as the explicit method, and the first and

second-order Euler methods as the implicit method. Note that in the first and second-order Euler methods, the sub-iteration number of the smallest computational time is adopted, and its sub-iteration number and the computational time are shown.

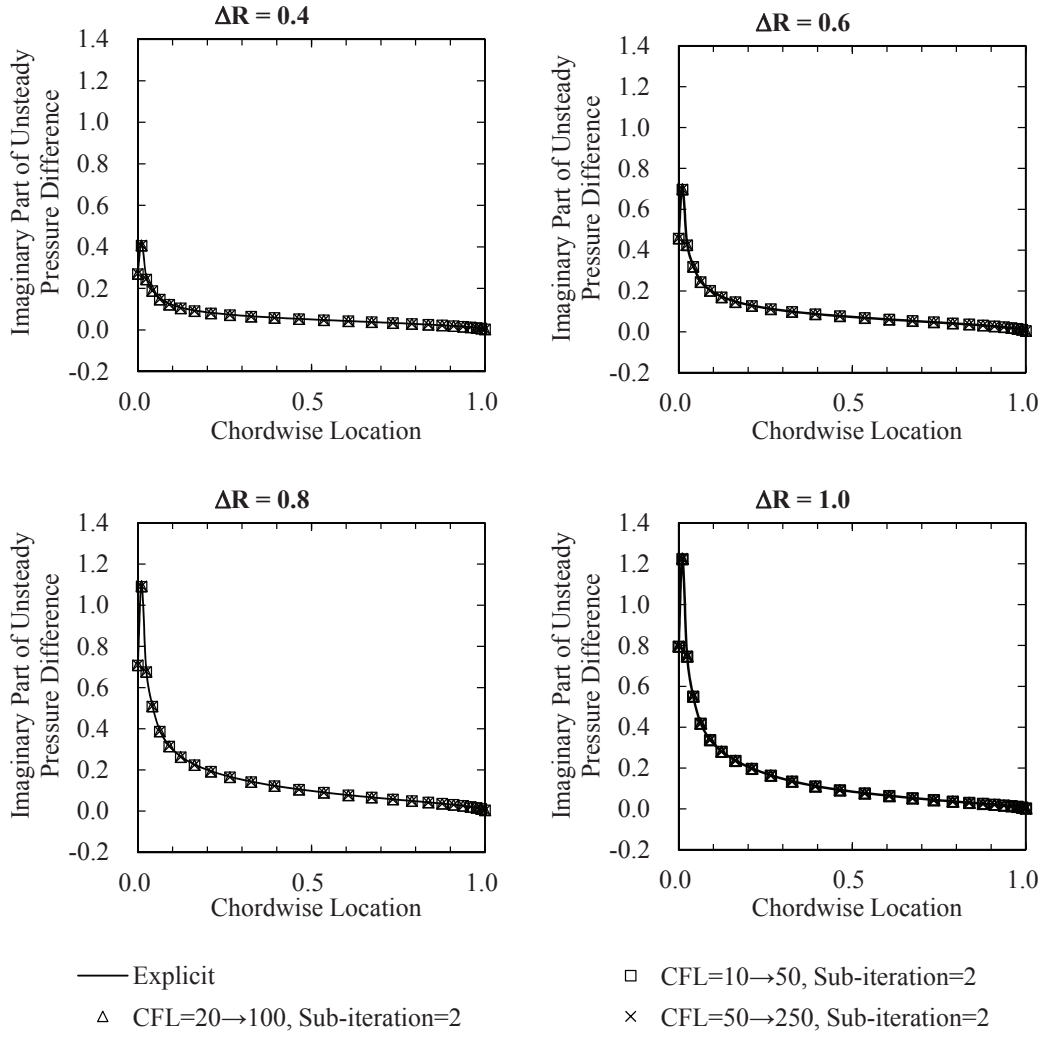

Fig. 3 Comparison of the imaginary part of unsteady pressure difference using the explicit and first-order Euler implicit methods

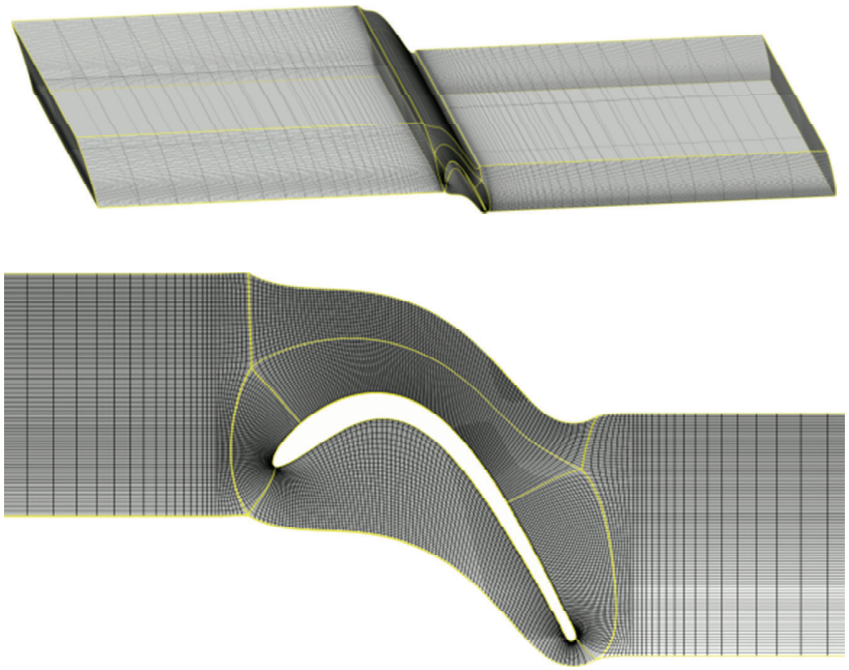

Fig. 4 Grids for low pressure turbine model

From Table 2, the computational time is 98.12 hours when the third-order Runge-Kutta method is used, while it is 0.56 hours when the first-order Euler method is used with CFL = 10→50 and 0.91 hours when the second-order Euler method is used with CFL=50→250. By using the implicit method, the computational time is reduced approximately by about 1/175 and 1/100 (two orders of magnitude smaller), when the first and second-order Euler methods are used, respectively.

Table 2 Comparison of the computational time in hours.

	CFL Number			
Time Integration Method	0.1 → 0.5	10 → 50	20 → 100	50 → 250
Third-order Runge-Kutta	98.12	-	-	-
First-order Euler	-	0.56, 2	0.64, 3	0.91, 15
Second-order Euler	-	2.96, 4	1.76, 8	0.91, 15

Figures 5 and 6 show the comparison of the unsteady pressure using the explicit method and the first and second-order Euler implicit methods, respectively, for the pressure and suction surfaces. The phase (argument) of 0 degrees corrresponds to the phase of vibration displacement. As is shown in Figs. 5 and 6, the correspondence of the numerical results using the explicit method and the first and second-order Euler implicit method is superb. Thus switching the time integration scheme from the explicit method to the implicit method enables the reduction in the computational time. The usage of the second-order Euler implicit method gives the same results, but requires nearly twice as much time as the usage of the first-order Euler method.

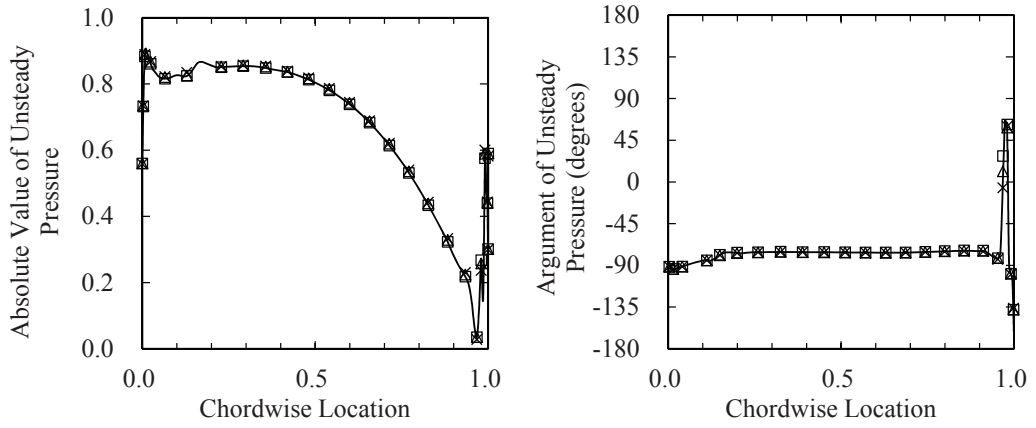

(a) Pressure Side

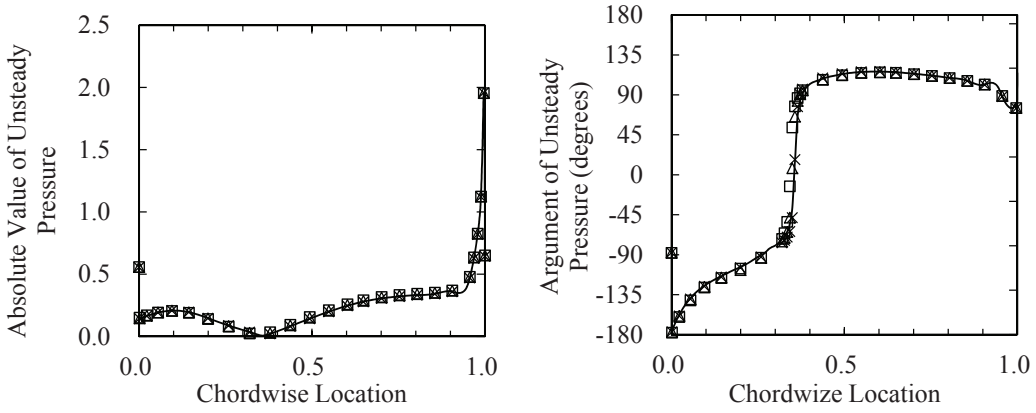

(b) Suction Side

Fig. 5 Comparison of the unsteady pressure using the explicit and first-order Euler implicit methods

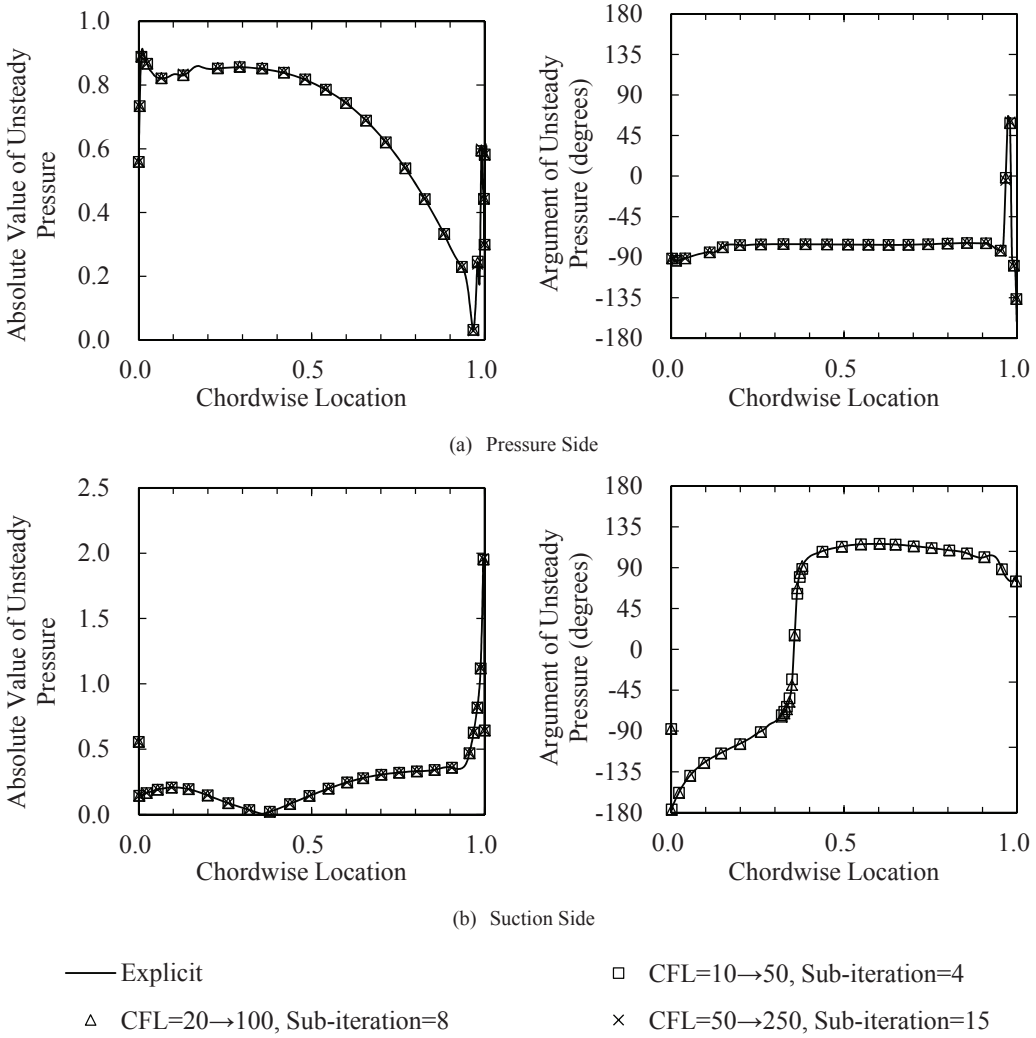

Fig. 6 Comparison of the unsteady pressure using the explicit and second-order Euler implicit methods

4. Conclusion

The unsteady pressure for the vibrating cascade blade row is numerically calculated using the implicit time integration methods. The main conclusions are as follows:

- The implicit time integration methods of the matrix free Gauss Seidel Method on the linear unsteady aerodynamics for the vibrating cascade blades are successfully established, and it is implemented in the code.

- The numerical results using the present implicit methods are compared with the results using the explicit third-order Runge-Kutta time integration method, and their correspondence is good.

- It is confirmed that the usage of the implicit methods instead of the explicit method reduces the computational time to the same degree of convergence by two orders of magnitude.

References

[1] Kubo, A., Yamasaki, N., and Aotsuka, M, Linear Unsteady CFD of a Vibrating Turbomachinery Blade Row, Proceedings of Asian Joint Conference on Propulsion and Power (AJCPP) 2012, AJCPP2012-033, CD-ROM, 2012.
[2] Shima, E., A Compressible CFD Method for Flow with Sound from Very Low Mach Number to Supersonic, BBAA VI International Colloquium on Bluff Bodies Aerodynamics and Applications, 2008.
[3] Namba, M., and Ishikawa, A., Three-Dimensional Aerodynamic Force Calculations of Oscillating Supersonic and Transonic Annular Cascades, ASME Journal of Turbomachinery, Vol. 105, pp. 138-146, 1983.